Proposal for Manipulating Functional Interface Properties of Composite Organic Semiconductors with Addition of Designed Macromolecules

P. Maniadis, T. Lookman, A. Saxena, and D. L. Smith

Manipulating functional interface properties of composite organic semiconductors

P. Maniadis, T. Lookman, A. Saxena, and D. L. Smith

Theoretical Division, Los Alamos National Laboratory, 87545 Los Alamos, NM, USA

The arrangement of the electronic levels in an interface between organic semiconductors is crucial for the operation of devices such as solar cells and light emitting diodes. With the addition of designed macro-molecules, we show that it is possible to control the relative position of the HOMO and LUMO levels, and consequently improve the performance. The designed macro-molecules consist of two end segments, each compatible with one of the interface components, and a central segment which adds functionality to the interface. The tails control the position and the orientation of the functional units. When the central functional unit is an electric dipole, an electrostatic field is created due to the orientation of the dipoles, which shifts the electronic levels in a controled way. We develop a theoretical framework, based on self-consistent field theory (SCF), to study the concentration and the orientation of the central functional units. We find that the levels can shift by as much as several tenths of an eV.

Organic semiconductors are of intrinsic scientific interest because strong competing interactions produce a rich spectrum of tunable ground and excited electronic states. These materials are technologically important for a broad class of applications because of the tunability of their electronic properties, their facile thin film and heterostructure fabrication, and the possibility of creating nanoscale structures and devices through molecular assembly techniques. Interfaces between two different organic semiconductors play a critical role in many devices [1–4]. For example, interfaces are used to achieve exciton dissociation in many organic solar cell designs and to control carrier transport in many organic light emitting diode designs [5–9]. In some organic device structures, planar interfaces are formed by subsequent thin film deposition techniques and in some device structures, such as bulk heterojunction solar cells, arrays of nonplanar interfaces are formed by phase segregation. The electronic structure of the interface determines the behavior of electronic processes that occur at the interface. An example of an important feature in the interface electronic structure is the relative positions of characteristic energies, such as the highest occupied molecular orbital (HOMO) and the lowest occupied molecular orbital (LUMO) levels, of the constituent interface components.

Self-assembled monolayer (SAM) techniques have been used to insert oriented electric dipole layers at planar metal/organic semiconductor interfaces. The oriented dipole layers were shown to shift the relative position of the metal Fermi energy and the organic semiconductor HOMO and LUMO levels by as much as several tenths of an eV [10, 11]. This interface energy shift was used to produce greatly improved charge injection properties at the metal/organic semiconductor interface. The molecules used for the SAMs had a thiol group at one end that attached to a noble metal electrode and an electron attracting or repelling group on the other end that produced the electric dipole moment. Because the thiol group bonded to the metal electrode, the dipole layer at the interface was oriented. This approach *is not applicable to nonplanar* bulk heterojunction interfaces formed by phase segregation.

Here we propose an approach to incorporate oriented molecular layers at the interface between two organic semiconductors that *does not require planar interfaces* and is appropriate for bulk heterojunction materials formed by phase segregation. We propose a systematic way to manipulate the electronic properties of these interfaces by the addition of designed macro-molecules containing a central functional segment. The long tails of the molecule serve to place the central functional unit at the interface and fix the orientation. An example of the central functional unit is an electric dipole which can manipulate interface electronic energy levels. We show that such oriented dipoles can be used to shift interface energy levels by as much as several tenths of an eV. This finding is based on a theoretical mean-field treatment [12–15] which allows for the study of concentration and orientation dependence of the central functional units.

We consider two conjugated polymer organic semiconductors labeled A and B that phase segregate when cast out of solution. We add to the mixture of A and B, the block copolymers A-C-B with the central functional C segment. The A and B tails of the macromolecule serve to place the central segment at the interface and to orient it with respect to the interface. Here we consider that C carries an electric dipole which will manipulate the electronic energy levels. Using self-consistent field theory (SCF) [12–15] we study the concentration and the orientation of the central functional units and calculate the average dipole moment and the standard deviation of the dipole moments from the average value. We find the important result that the interface energy levels can be shifted in a controlled manner by as much as $0.3\ eV$.

For simplicity we take the A and B polymers to have the same degree of polymerization N, while the A-C-B molecules have a degree of polymerization M which may differ from N. We take the same number n of polymer chains of type A and B, and a different number m of chains of type A-C-B. For the model details and calcula-

tions see [16, 17].

The basic SCF theory and the numerical methods for the solution of the resulting field equations are described in detail elsewhere [12–16]. Here we highlight the basic equations, and *extend the theory to calculate new fields* such as the orientation of the C-segments in the vicinity of the interface. The interaction of neighboring monomers in the same polymer chain is described using the Gaussian chain model with elastic energy H_0, and the incompatibility between different types of monomers is described by the Flory-Huggins energy H_1. $\alpha = M/N$ is the ratio of the degree of polymerization of the A-C-B and A or B polymers. The functional units C are small conjugate chain, with length M_C, the side chain of length M_A of type A, attached on one side located at $s = f_a$, and a similar chain of type B on the other side with $M_B = M_A$ at $s = f_b$ (s is the normalized contour length of the polymer). There is a polar side group attached on each side of the middle segment C that add a negative electric charge $-q$ close to the A-C bond and a positive charge $+q$ close to the C-B bond as we show in Fig. 1(a). The concentration of C increases in the vicinity of the interface, and due to the attachments, the dipoles will have an average orientation from the A-domain towards the B-domain (Fig. 1a,b). The orientation of the electric dipoles will create an electrostatic field, which will shift the HOMO and LUMO levels of the conjugate polymers as depicted schematically in Fig. 1(c,d,e).

For the electrostatic interactions we introduce the charge densities [18, 19] $\hat{Q}^- = -q \sum_{l=1}^{m} \delta(\mathbf{r} - \mathbf{R}_C^l(f_a))$, $\hat{Q}^+ = +q \sum_{l=1}^{m} \delta(\mathbf{r} - \mathbf{R}_C^l(f_b))$, and the total charge density then is given by $\hat{\rho}_e = \hat{Q}^- + \hat{Q}^+$. We also introduce the electrostatic energy density

$$H_2 = \int d\mathbf{r} \left\{ \hat{\rho}_e \Psi(\mathbf{r}) - \frac{\epsilon}{8\pi} |\nabla \Psi|^2 \right\}, \quad \text{(CGS)} \quad (1)$$

where $\Psi(\mathbf{r})$ is the electrostatic potential, and ϵ is the dielectric susceptibility of the polymer system. The second term in Eq. (1), with the minus sign, corrects for double counting in the first term. In our formal structure, it is convenient to use this form for the electrostatic energy density.

The partition function and the free energy of the system is calculated using SCF, and the mean values are calculated at the saddle node approximation [12–19]. The resulting equations are solved self-consistently to find the monomer and charge densities. We normalize the densities by dividing by the average monomer density ρ_0, therefore Φ_i is the normalized density of monomers of type i, ω_i is the related conjugate chemical potential field, $\chi_{i,j}$ is the Flory-Huggins incompatibility parameter between species i and j, with $\Phi_A + \Phi_B + \Phi_C = 1$.

We introduce the dimensionless charge density $\Phi_q = \rho_e/q$ and the electrostatic field $\Psi' = q\Psi$, which affect the source term of the diffusion equation at the end points of the functional unit C, where there is the electrostatic

charge. Minimization of the free energy with respect to the electrostatic fields and densities gives a Poisson's equation to be solved self-consistently together with the polymer equations $\nabla^2 \Psi' = -(A/M)\Phi_q$, where M is the degree of polymerization of the A-C-B polymer chains, and the constant A contains the other polymer and electrostatic quantities (density, local charge, permeability etc) $A = q^2(4\pi\rho_0/\epsilon)$. We have estimated the value of this constant for PPV, to be $A \simeq 50 \ eV \ monomer/nm^2$ assuming that the electronic charge at the ends of the functional unit is $\pm e$.

For every A-C-B molecule we assign a dipole moment $\vec{d_l} = d_0 \ (\ \vec{R}_l(f_b) - \vec{R}_l(f_a) \ )$ (where $s = f_b$ is the head of C, and $s = f_a$ the tail of C). For small C segment we can assign this dipole moment at a particular point in space $\vec{R}_l(m)$ where $s = m$ at the middle of C. Based on this definition, we get the distribution of dipole moments for a particular molecular configuration, $\hat{D}(\vec{r})$ and the moment from all A-C-B molecules

$$\hat{D}(\vec{r}) \ = \ \sum_l \vec{d_l} \ \delta(\vec{r} - \vec{R}(m_l)). \qquad (2)$$

The average field distribution of the dipole moments corresponds to the statistical average of this vector field calculated over all possible realizations [20]. We use the field theory approach for the calculation of this statistical average, applying the Hubbard-Stratonovich transformation. Here we derive an expression for the field dipole distribution $\vec{D}(\vec{r}) = \langle \hat{D}(\vec{r}) \rangle$ using the SCF theory (for the detailed calculation see [16, 17]). In addition, we derive the expression for the second moment of the distribution of the dipole vectors $\sigma_D^2(\vec{r})$.

For the numerical solution of the SCF equations we fix the degree of polymerization of the A and B homopolymer chains to $N = 1000$ and the length of the functional unit $M_C = 40$, while the length of the A and B attachments $M_A = M_B$ varies, depending on the simulation. We performed numerical simulations for different values of the Flory-Huggins incompatibility parameters, here we present typical behavior of the system for $\chi_{AB} = 6$ which is sufficient for the formation of the interface in A/B blends (perpendicular to the x-direction). We also set $\chi_{AC} = \chi_{BC} = 0$, the results remain qualitatively the same for small variations of χ_{AC} and χ_{BC}. The simulations are performed in a square 64×64 lattice with periodic boundary conditions.

In Fig. 2(a,b) we plot the calculated density of the three components Φ_A, Φ_B, Φ_C, and the dipole moment $D_x(\mathbf{r})$ for $M_A = M_B = 450$ (Fig 2c). As seen in the figure, the functional units C have a higher concentration in the vicinity of the A/B interface. This increase in Φ_C at the interface reduces the enthalpic repulsion between A and B, and therefore minimizes the total free energy. Due to the tails attached on the functional units, the C dipoles have an average orientation in a direction perpendicular to the interface. The orientation and the fluctuations of

the dipoles are calculated using the field equation derived from equation (2). In Fig. 2(c) we present the average orientation of the dipoles, the arrows indicate the direction of the dipoles (left to right for positive, and right to left for negative values).

The average orientation of the dipoles in a direction perpendicular to the interface leads to an electrostatic charge density distribution in the material, due to the $\pm q$ charge on the two ends of the C-segment. Solving the Poisson's equation we find that there is an electrostatic field Ψ' difference between the A and B domains, which is of order $0.3 \, eV$. In Fig. 2(d) we show the electrostatic field Ψ' (for the same parameters as in Fig. 2(a,b)). In Fig. 2(e) we show the density of the electric charges Φ_q. We see that there is an accumulation of positive charge ($\Phi_q > 0$) in the B domain, and a negative charge ($\Phi_q < 0$) in the A domain, which creates the electrostatic field difference shown in Fig. 2(d).

In Fig. 3(a) we show the variation of the average orientation of the dipoles as a function of the length of the attachments $M_A = M_B$. The entropic and enthalpic forces on the dipoles increase, as the length of the attachment increases, which affects both the concentration and the orientation of the C segments. The result as we show in this figure, is that the dipole moment increases with the length of the attachments which leads to an increase of the charge density distribution, and the electrostatic field variation between the two domains. In Fig. 3(b) we plot the potential difference $\Delta\Psi'$ between the A and B domains as a function of the length of the attachments (in monomer units).

As seen in Fig. 4(a), the orientation of the dipoles (and therefore the electrostatic field) is affected by the relative concentration of the functional units. As the volume fraction v_C of molecules of type A-C-B is increased, the number of dipoles in the vicinity of the interface increases, and therefore there is an increase in the dipole moment and the electrostatic potential. This increase continues until the relative volume fraction is of order 0.3. For volume fractions larger than this value, the dynamics of the A-C-B molecules start to influence the structure of the interface, making it wider, and therefore it effectively reduces the C concentration, while at the same time it increases the fluctuations σ^2. For volume fractions of the order of 0.7, the interface is destroyed, and the dipoles are uniformly distributed with random orientation.

The deviation of the distributions of dipoles σ^2 as a function of the volume fraction is plotted in Fig. 4(b). Due to the concentration of the dipoles at the interface, for $v_C < 0.3$ the deviation is almost zero in the middle of the A or B domains, while it has a small value on the interfaces. This means that the distribution of dipole orientations is small. When the volume fraction becomes larger than $v_C > 0.3$, the interface becomes wider, which results in a wider distribution of the orientation of dipoles (with larger values of σ^2). For larger values of the volume

fraction, the interface is destroyed, and we find a uniform distribution of dipole orientations, with large values of σ^2.

In conclusion, interfaces between organic semiconductors are essential for the operation of a wide range of organic semiconductor devices. We have shown that the electronic properties of these interfaces can be manipulated by introducing designed macro-molecules consisting of two end segments, each compatible with one of the interface components, and a central segment which adds functionality to the interface. The concentration and orientation of the functional units is controlled by the attachment tails. We developed a mean field theory to study the position, orientation and statistical fluctuations of the functional units. For the specific case of electrostatic dipoles as functional units, we find that the HOMO and LUMO levels of the constituent organic semiconductors can be adjusted by as much as several tenths of an eV. These results provide an exciting new interface design strategy for organic semiconductor devices, in particular bulk heterojunctions.

Acknowledgments

[1] G. Yu, J. Gao, J. C. Hummelen, F. Wudl, and A. J. Heeger, Science **270**, 1789 (1995).
[2] G. Yu, J. Wang, J. McElvain, A. J. Heeger, Adv. Mat. **10**, 1431 (1998).
[3] C. W. Tang, and S. A. Van Slyke, Applied Physics Letters **51**, 913-915 (1987).
[4] J. H. Burroughes, et al. Nature **347**, 539 (1990).
[5] P. W. M. Blom, V. D. Mihailetchi, L. J. A. Koster, D. E. Markov, D. E. Advanced Materials **19**, 1551-1566 (2007).
[6] R. A. Marsh, J. M. Hodgkiss, and R. H. Friend, Advanced Materials **22**, 3672-3676 (2010).
[7] H.P. Park, et al. Nature Photonics **3**, 279-303 (2009).
[8] C. Lombardo, and A. Dodabalapur, Applied Physics Letters **97**, 233302 (2010).
[9] H. Ohkita, et al. J. Am. Chem. Soc. **130**, 3030-3042 (2008).
[10] I. H. Campbell, S. Rubin, T. A. Zawodzinski, J. D. Kress, R. L. Martin, D. L. Smith, N. N. Barashkov, and J. P. Ferraris, Phys. Rev. B **54**, R14321 (1996).
[11] I. H. Campbell, J. D. Kress, R. L. Martin, D. L. Smith, N. N. Barashkov, and J. P. Ferraris, Appl. Phys. Lett. **71**, 3528 (1997).
[12] M. W. Matsen, J. Phys.: Cond. Mat. **14**, R21 (2002).
[13] G. F. Fredrickson, V. Ganesan, and F. Drolet, Macromolecules **35**, 16 (2002).
[14] P. Maniadis, R. B. Thompson, K. ØRasmussen, and T. Lookman, Phys. Rev. E **69**, 031801 (2004).

[15] G. Tzeremes, K. Ø. Rasmussen, T. Lookman, and A. Saxena, Phys. Rev. E **65**, 041806 (2002).

[16] P. Maniadis, T. Lookman, A. Saxena, and D. L. Smith, Phys. Rev. B, preprint (2012).

[17] P. Maniadis, T. Lookman, A. Saxena, and D. L. Smith, supplementary material.

[18] An-G. Shi, and J. Noolandi, Macromol. Theory Simul. **8**, 214 (1999).

[19] Q. Wang, T. Taniguchi, and G. H. Fredrickson, J. Phys. Chem. B 2004, **108**, 6733 (2004).

[20] M. Doi, M. and S. F. Edwards, "The theory of polymer dynamics", Oxford University Press, New York (1986).

Figures

FIG. 1: Schematic representation of the polymer structure, the interface and the electronic levels. (a) The polymers, A, B, and the macromolecule A-C-B, (b) schematic diagram of the oriented macromolecules concentrated at the interface, (c) HOMO and LUMO electronic levels of the A/B interface, (d) shifted HOMO and LUMO levels in the presence of oriented electric dipoles, with $-q$ in the A domain, and $+q$ in the B domain, (e) shifted HOMO and LUMO levels with dipole orientation opposite that (d).

FIG. 2: Monomer densities, dipole moment, electrostatic potential and charge density as a function of position: (a) Φ_A and Φ_B, (b) Φ_C, (c) x component of the dipole moment $D_x/d_0 R_g$, (the arrows indicate the average direction of the C dipoles), (d) electrostatic potential (in eV), (e) normalized charge distribution Φ_q (lower panel) as a function of position.

FIG. 3: (a) Calculated x-component of the dipole moment $D_x/d_0 R_g$ as a function of position and the length of the chains attached to the functional unit $M_A = M_B$, (b) calculated difference in the electrostatic potential $\Delta \Psi'$ in eV, as a function of the length of the chains attached to the functional unit $M_A = M_B$.

FIG. 4: (a) Calculated x-component of the dipole moment $D_x/d_0 R_g$ as a function of position and the volume fraction of the functional units, (b) calculated standard deviation $\sigma^2/d_0^2 R_g^2$ of the orientation of the dipoles from the average value, as a function of position and the volume fraction of the functional units.
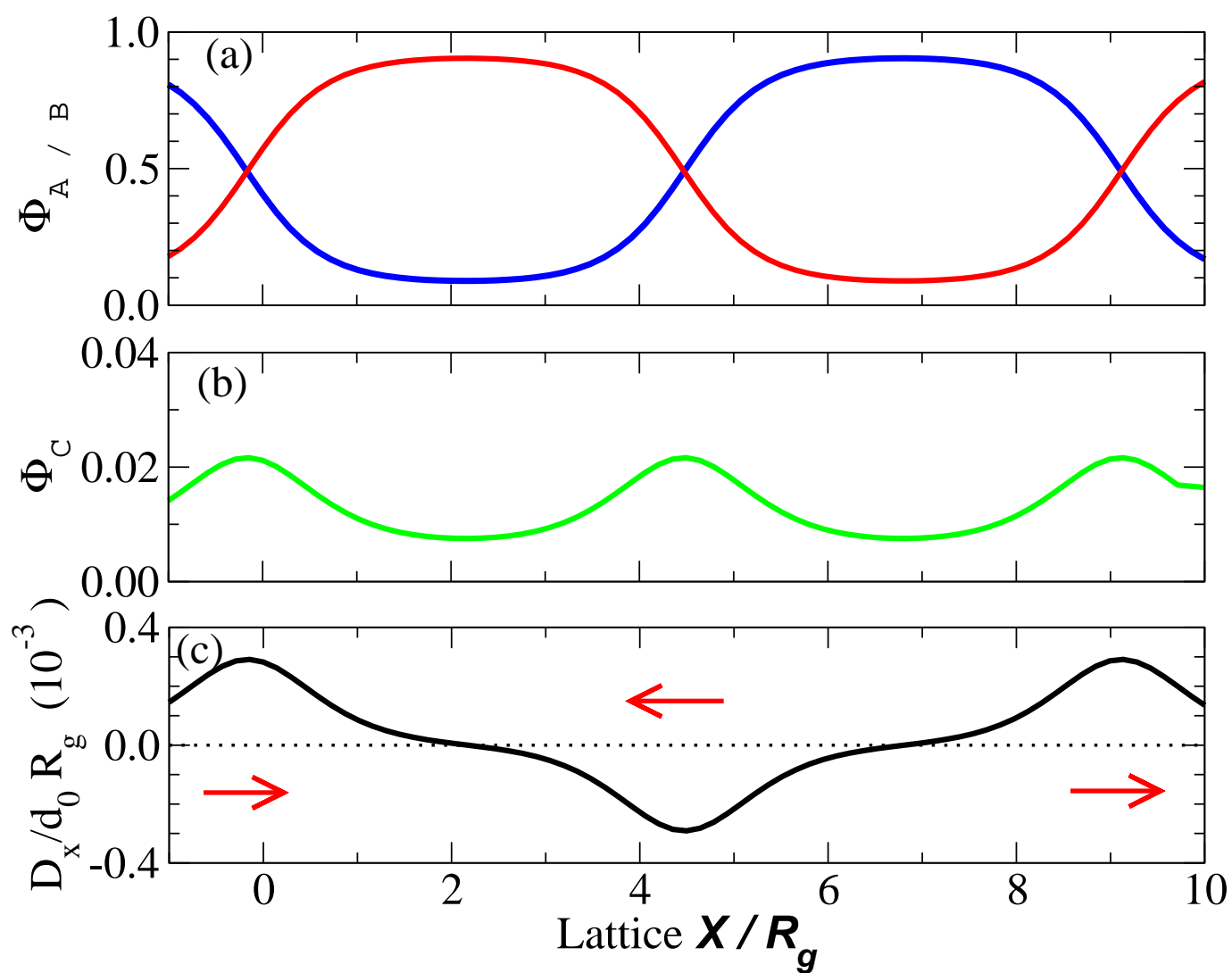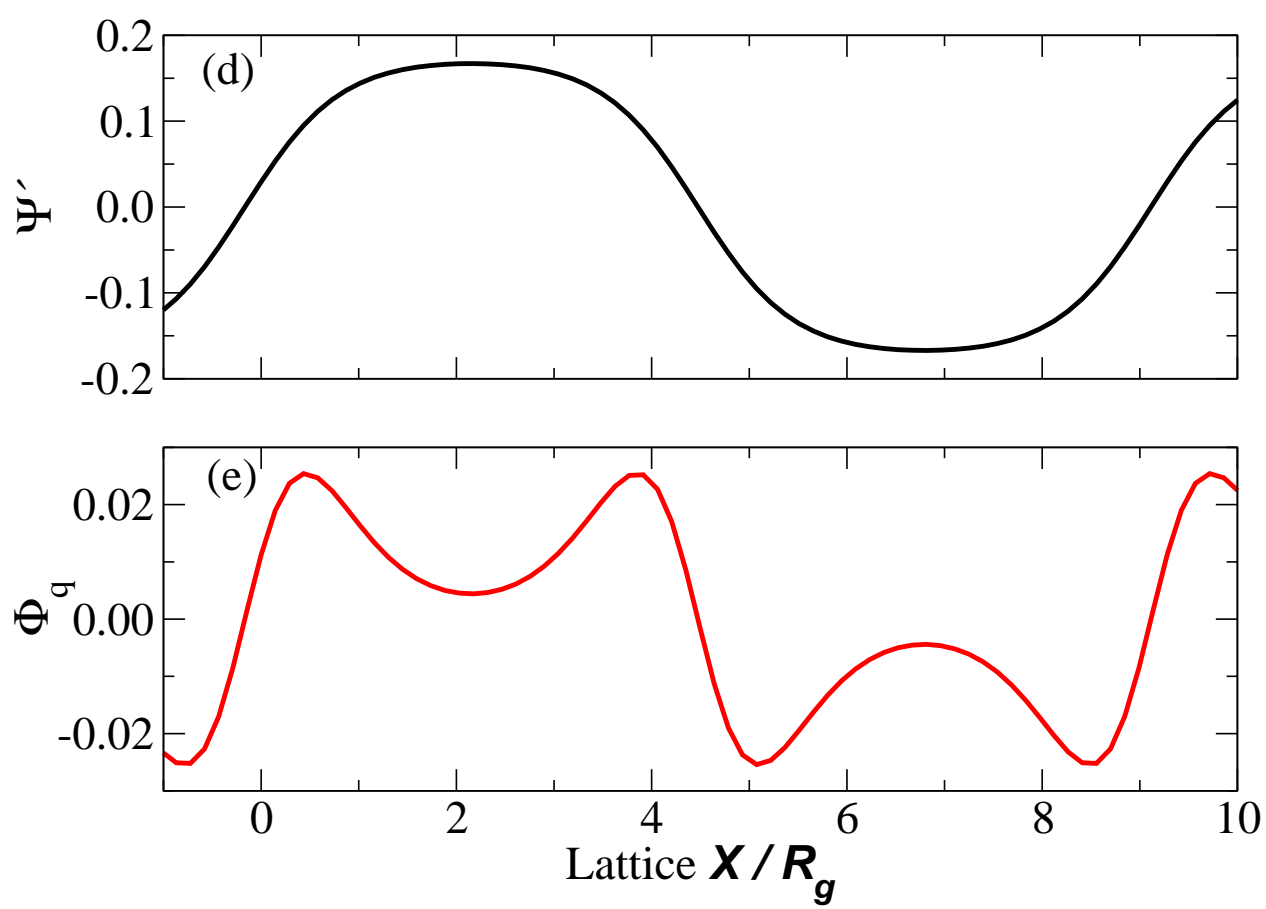
(a)

A

B

A
−q +q
B
$\vec{C}$

(b)

A   B

(c) A   B

⊖

LUMO

HOMO ⊕

(d)

$\vec{D}$ →
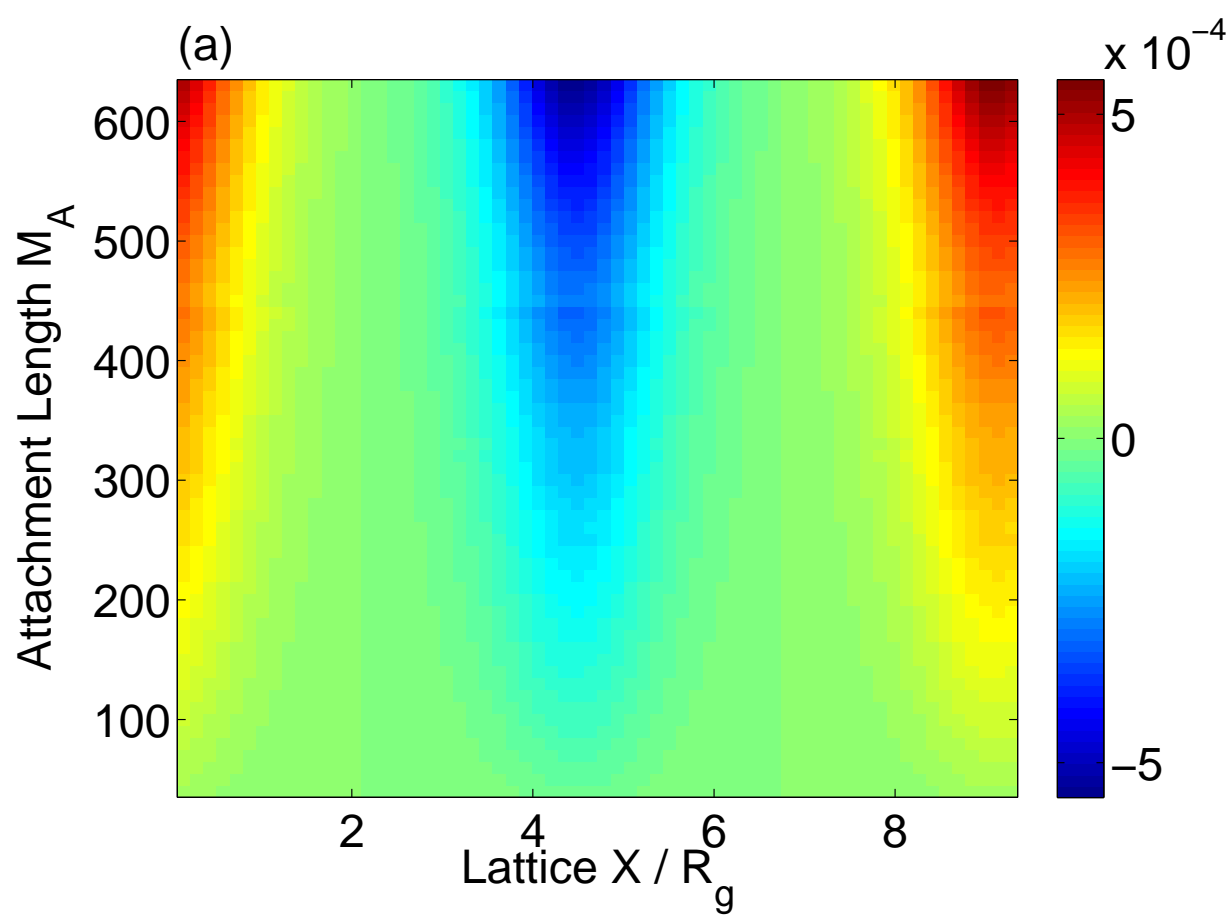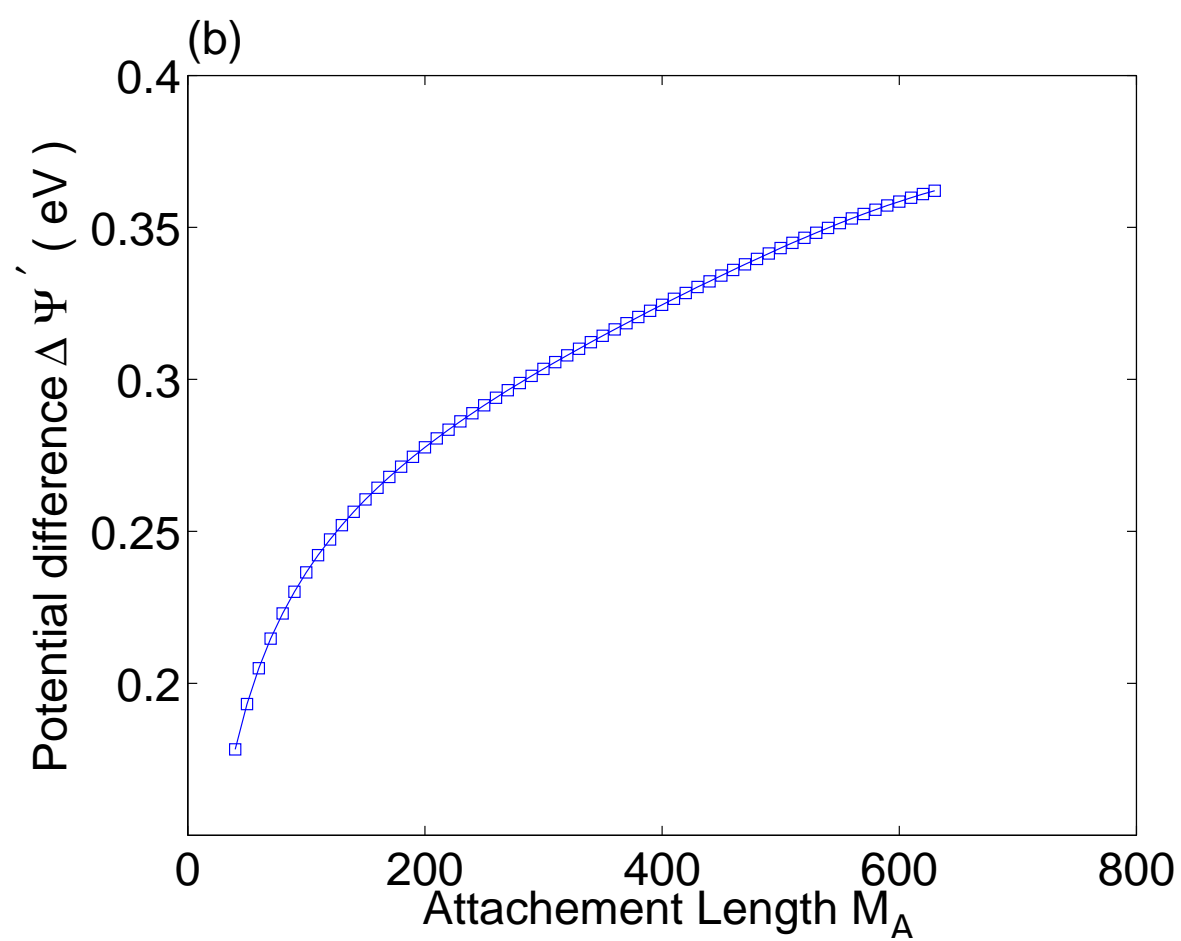
(e)

← →
$\vec{D}$
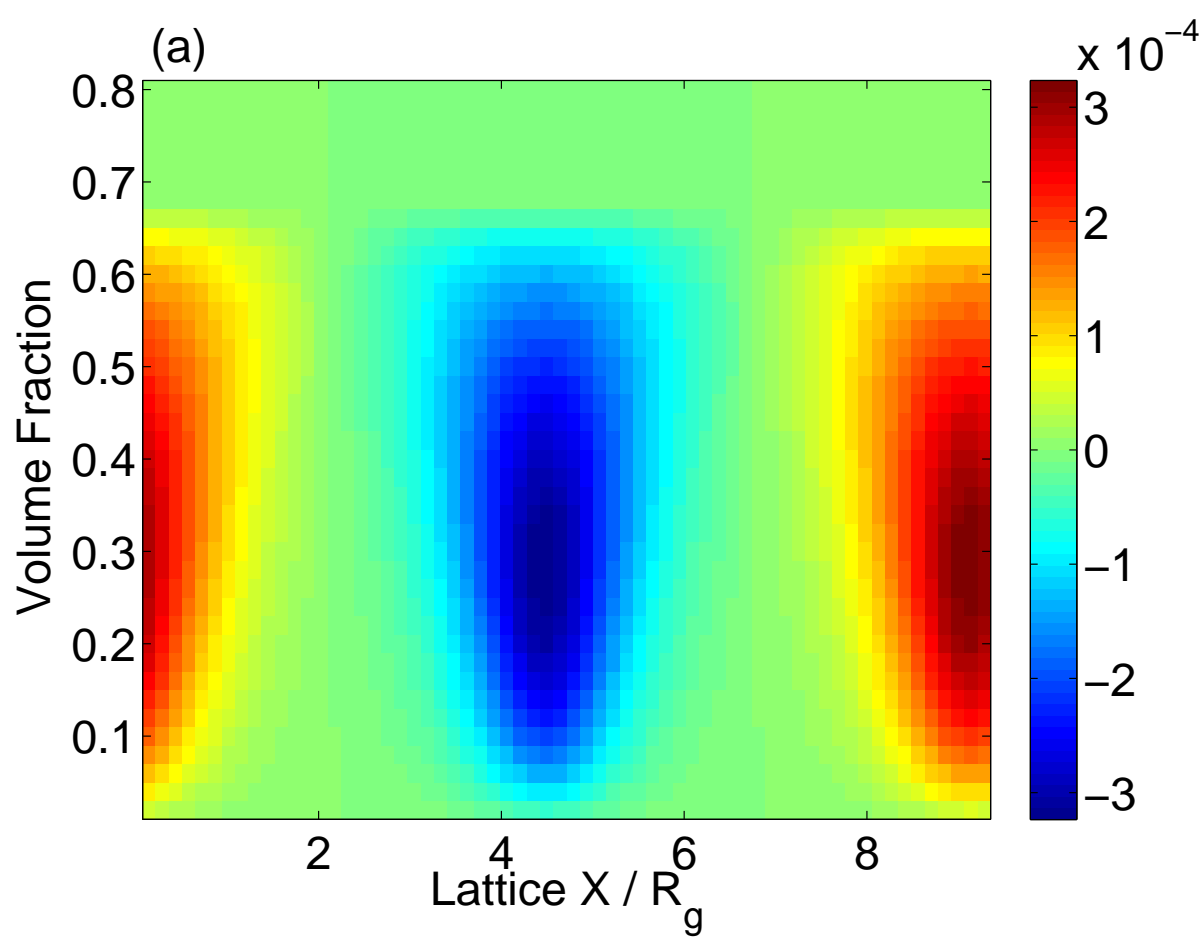
Figure 1   LN13074   10Apr2012
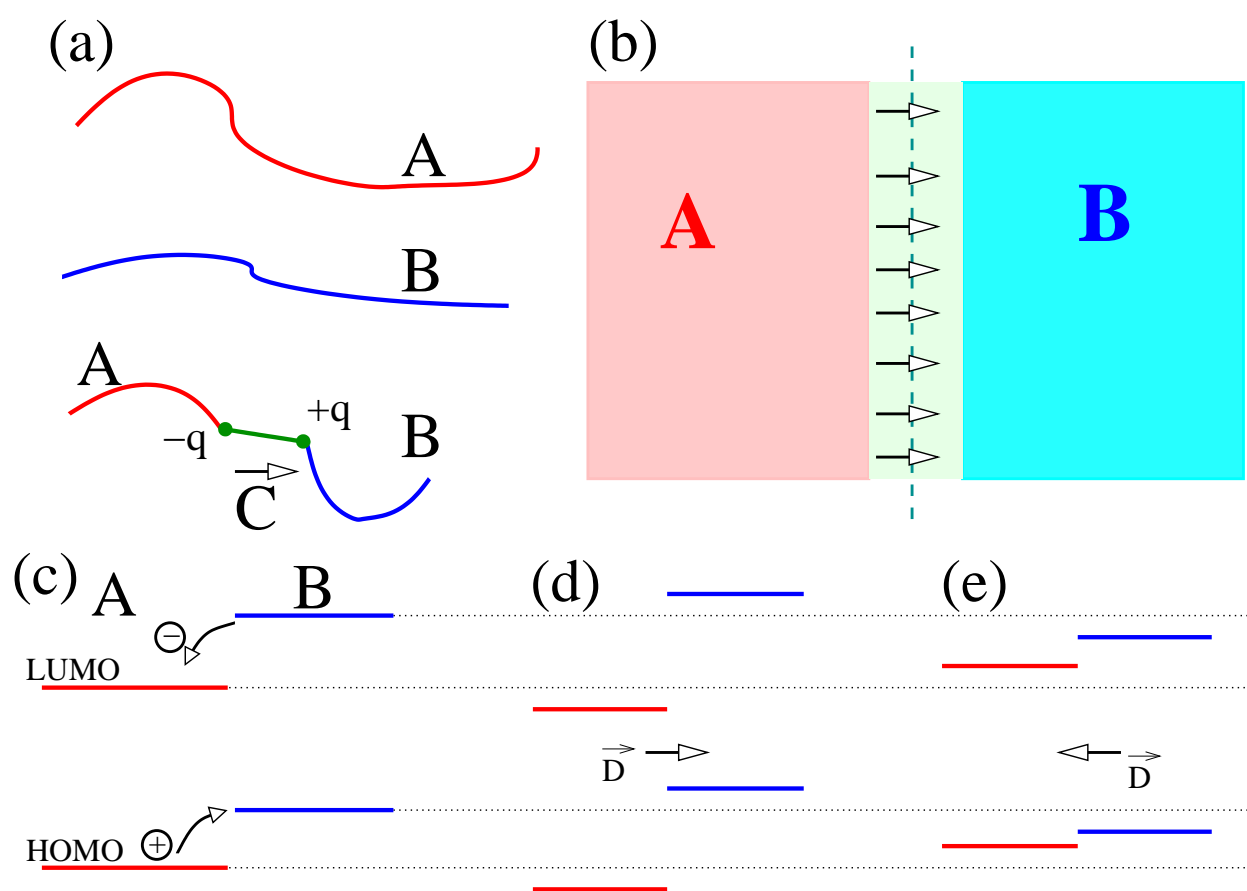
Figure 2a   LN13074   10Apr2012

Figure 2b   LN13074   10Apr2012

(a)

x 10^{-4}

Attachment Length M_A

Lattice X / R_g

Figure 3a   LN13074   10Apr2012

Figure 3b   LN13074   10Apr2012
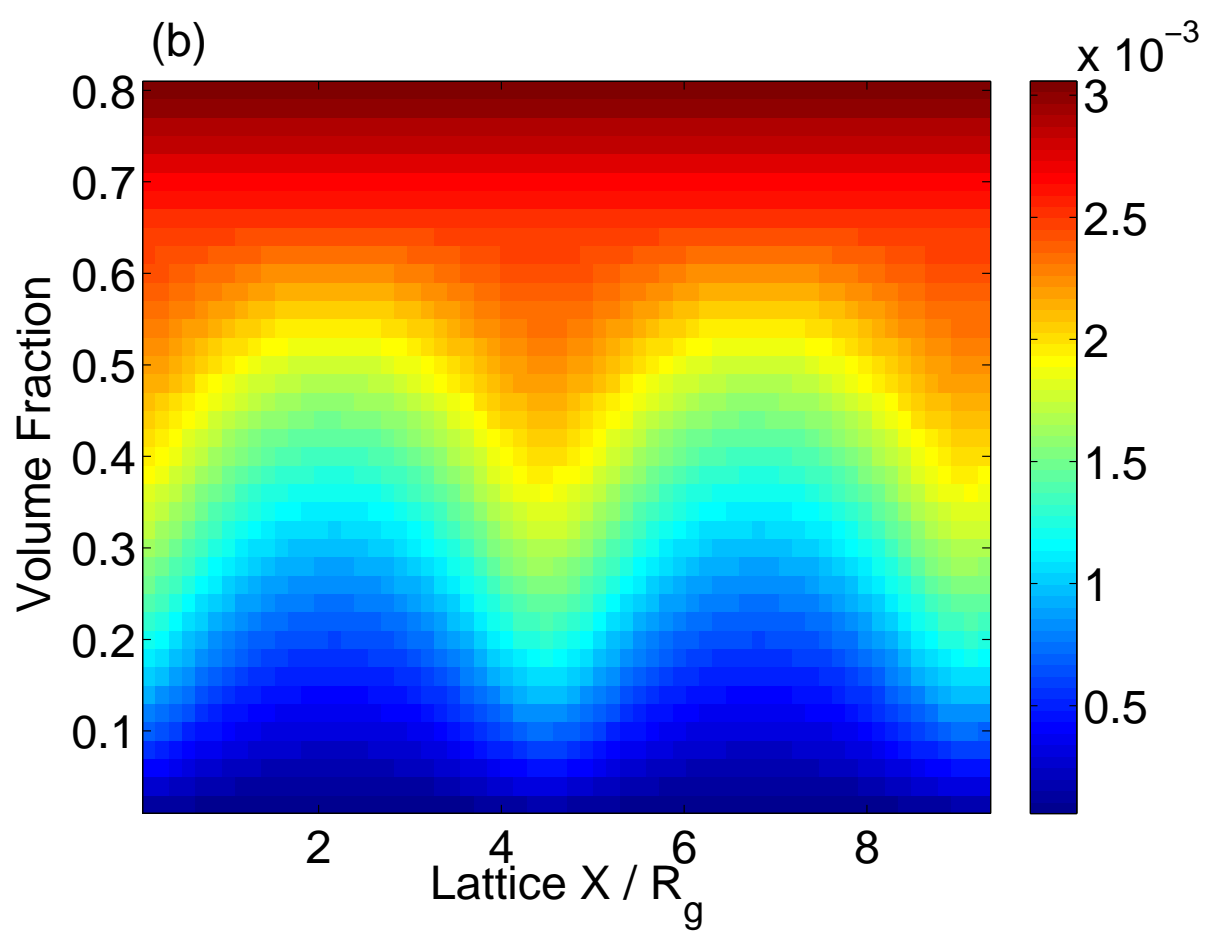
(a)

x 10^{-4}

Volume Fraction

Lattice X / R$_g$

Figure 4a   LN13074   10Apr2012

(b)

Figure 4b   LN13074   10Apr2012